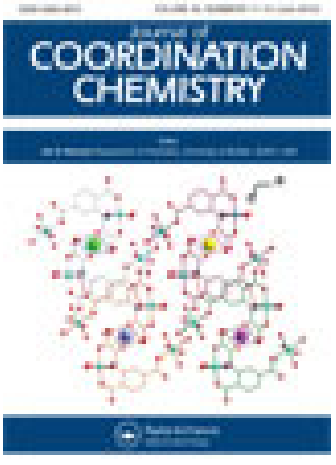


Journal of Coordination Chemistry
Publication details, including instructions for authors and subscription information:
http://www.tandfonline.com/loi/gcoo20

# Different hydrogen-bonding patterns in two [Zn(ENTPP)] complexes with water or methanol as ligands

Weiguang Fang [a b], Jiaxun Jiang [a], Hong Yu [a], Wen Yang [a], Xiaoming Ren [b] & Chuanjiang Hu [a a]

[a] Key Laboratory of Organic Synthesis of Jiangsu Province, College of Chemistry, Chemical Engineering and Materials Science, Soochow University, Suzhou 215123, P.R. China

[b] College of Science, Nanjing University of Technology, Nanjing 210009, P.R. China

Published online: 10 May 2012.

To cite this article: Weiguang Fang, Jiaxun Jiang, Hong Yu, Wen Yang, Xiaoming Ren & Chuanjiang Hu (2012) Different hydrogen-bonding patterns in two [Zn(ENTPP)] complexes with water or methanol as ligands, Journal of Coordination Chemistry, 65:11, 1905-1914, DOI: 10.1080/00958972.2012.686035

To link to this article: http://dx.doi.org/10.1080/00958972.2012.686035

*Journal of Coordination Chemistry*
Vol. 65, No. 11, 10 June 2012, 1905–1914



# Different hydrogen-bonding patterns in two [Zn(ENTPP)] complexes with water or methanol as ligands

WEIGUANG FANG†‡, JIAXUN JIANG†, HONG YU†, WEN YANG†, XIAOMING REN‡ and CHUANJIANG HU*†

†Key Laboratory of Organic Synthesis of Jiangsu Province, College of Chemistry, Chemical Engineering and Materials Science, Soochow University, Suzhou 215123, P.R. China
‡College of Science, Nanjing University of Technology, Nanjing 210009, P.R. China

(*Received 6 January 2012; in final form 12 March 2012*)

We have synthesized zinc complexes of $H_2$ENTPP (5-(8-ethoxycarbonyl-1-naphthyl)-10,15,20-triphenyl porphyrin) as a model to study hydrogen-bonding interactions. When water or methanol is a ligand, crystals of [Zn(ENTPP)($CH_3OH$)] or [Zn(ENTPP)($H_2O$)] · $C_6H_5CH_3$ were obtained. In both structures, the ligand has hydrogen-bonding interactions, but in different patterns. In [Zn(ENTPP)($CH_3OH$)], the methanol oxygen and carboxylate oxygen in the naphthyl group form an intermolecular hydrogen bond. In [Zn(ENTPP)($H_2O$)] · $C_6H_5CH_3$, there are two independent molecules A and B. In molecule B, there is an intramolecular hydrogen bond between the water oxygen and the carboxylate oxygen, while in molecule A, besides the intramolecular hydrogen bond, there is an intermolecular hydrogen bond between the water oxygen and the carboxylate oxygen. $^1$H NMR spectra suggest the binding of methanol or water to zinc are equilibrium processes in solution. Equilibrium constant has been determined by UV-Vis measurements, and it suggests the binding affinity of zinc to methanol has been moderately increased.

*Keywords*: Porphyrin; Hydrogen bond; Naphthyl; Binding constant



## 1. Introduction

Hydrogen-bonding interactions are common in biological systems and model systems. In chiral recognition processes, such interactions play important roles in porphyrin-based systems, such as in a mono-porphyrin system reported by Ogoshi and coworkers [1, 2]. This system contains both a coordination site and a hydrogen-bonding site, so the host is capable of binding amino acid esters, through a two-point fixation mechanism, i.e., amine/zinc coordination and ester carbonyl/naphthol hydrogen-bonding, leading to effective chiral recognition of amino acid esters. Hydrogen-bonding can also affect the recognition ability. For example, in 5,15-bis(2-hydroxy-1-naphthy1) octaethylporphyrin reported by Aoyama *et al*. [2], there is a remarkable difference in binding constants between the *trans* and *cis* isomers. So it is important to synthesize new

*Corresponding author. Email: cjhu@suda.edu.cn

*Journal of Coordination Chemistry*
ISSN 0095-8972 print/ISSN 1029-0389 online © 2012 Taylor & Francis
http://dx.doi.org/10.1080/00958972.2012.686035

porphyrin-based hydrogen-bonding systems and study the corresponding hydrogen-bonding interactions.

We are interested in hydrogen-bonding interactions in model systems [3] and have recently studied the intramolecular hydrogen-bonding on the structure of a porphyrin [Zn(SATPP)($CH_3OH$)] (SATPP, dianion of 5-(2-salicylideneaminophenyl)-10,15,20triphenylporphyrin) [4]. One of our ongoing projects is to study chiral recognition in porphyrin systems containing hydrogen-bonding interactions. Recently, we designed a porphyrin, 5-(8-ethoxycarbonyl-1-naphthyl)-10,15,20-triphenyl porphyrin ($H_2$ENTPP), as shown in scheme 1 [5]. Its metal complex could provide a coordination site, a hydrogen-bonding site and a steric interaction site, as a potential host in chiral recognition. In this article, we have synthesized two zinc complexes, [Zn(ENTPP)($CH_3OH$)] and [Zn(ENTPP)($H_2O$)]$\cdot C_6H_5CH_3$, and studied hydrogen-bonding interactions in their solid structures. Binding constant of zinc to methanol has also been determined by UV-Vis measurements.



## 2. Experimental

### 2.1. *General procedures*

**2.1.1. Materials and general methods.** All reagents were of analytical grade and used without purification. All solvents were used as received. $^1$H NMR spectra were carried out using a Bruker AVANCE 400 spectrometer.

### 2.2. *Synthesis of [Zn(ENTPP)]*

[Zn(ENTPP)] was prepared according to literature procedure [6]. A solution of $Zn(CH_3COO)_2\cdot 2H_2O$ (0.125 g, 0.57 mmol) in methanol (5 mL) was added to the solution of $H_2$ENTPP (0.21 g, 0.28 mmol) in chloroform (50 mL). The mixture was refluxed for 3 h. After completion of the reaction, the solution was washed with water ($3\times 100$ mL). The organic layer was collected, then dried over magnesium sulfate, and concentrated under reduced pressure. The residue was purified on silica gel with methylene chloride/hexane (1 : 1) to give light purple solid. Yield 0.20 g (89%).

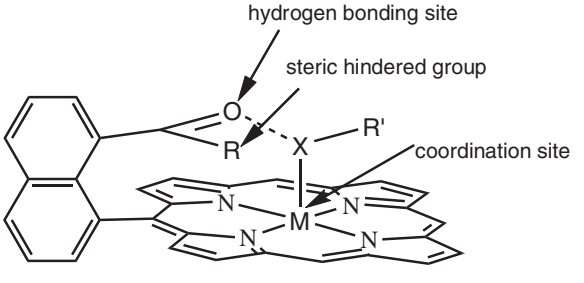


Scheme 1 A potential host for chiral recognition.

Anal. Calcd for $C_{51}H_{34}N_4O_2Zn \cdot 0.5H_2O$ (%): C, 75.69; H, 4.36; N, 6.92. Found: C, 75.54; H, 4.29; N, 6.87.

### 2.3. *X-ray crystallography*

Suitable crystals of [Zn(ENTPP)($CH_3OH$)] for X-ray diffraction were grown from diffusion of methanol into the toluene solution in 8 mm diameter glass tubes. When methanol was replaced by hexane, X-ray quality crystals of [Zn(ENTPP)$H_2O$] · $C_6H_5CH_3$ were obtained.

X-ray data collection was made on a Rigaku Mercury CCD X-ray diffractometer using graphite monochromated Mo-K$\alpha$ radiation ($\lambda = 0.071073$ nm) at 223(2) K for [Zn(ENTPP)($CH_3OH$)] and at 293 K for [Zn(ENTPP)($H_2O$)] · $C_6H_5CH_3$. Both crystals were solved by direct methods and refined on $F^2$ using full-matrix least-squares with SHELXTL version 97 [7]. Anisotropic thermal parameters were refined for non-hydrogen atoms. Hydrogen atoms, H(1 S) in [Zn(ENTPP)$CH_3OH$], H(1WA), H(2WA), H(1WB), and H(2WB) in [Zn(ENTPP)($H_2O$)] · $C_6H_5CH_3$, were found in Fourier maps, their coordinates and isotropic temperature factors were refined; other hydrogen atoms were theoretically added riding on their parent atoms. In the structure of [Zn(ENTPP)($H_2O$)] · $C_6H_5CH_3$, toluene was disordered over two positions and both were refined as rigid groups. After the final refinement the occupancy of the major orientation was 64%. Crystal data for [Zn(ENTPP)$CH_3OH$] and [Zn(ENTPP)($H_2O$)] · $C_6H_5CH_3$ are listed in table 1.

### 2.5. *Equilibrium constant determination*

UV-Vis spectra were measured on a Shimadzu UV-3150 spectrometer. Microliter amounts of freshly distilled methanol were added to $1.78 \times 10^{-6}$ mol $L^{-1}$ [Zn(ENTPP)] in $CH_2Cl_2$. The concentrations of methanol for UV-Vis measurements ranged from $1.85 \times 10^{-3}$ to $1.23 \times 10^{-1}$ mol $L^{-1}$. Absorbance changes were monitored by observing the increase in intensity of the Soret band at 422 nm.

## 3. Results and discussion

### 3.1. *Molecular structure*

The porphyrin complex has been synthesized by mixing $H_2$ENTPP with methanol solution of $Zn(CH_3COO)_2 \cdot 2H_2O$. In the presence of methanol, X-ray quality crystals of [Zn(ENTPP)($CH_3OH$)] were crystallized; while in the absence of methanol, crystals of [Zn(ENTPP)($H_2O$)] · $C_6H_5CH_3$ were obtained, such coordinated water is probably in the original toluene/hexane solvent. Both structures have been determined by X-ray crystallography.

The crystal structure of [Zn(ENTPP)($CH_3OH$)] has been solved in the $P2(1)/c$ space group, and one asymmetric unit consists of one zinc porphyrinate molecule. The crystal structure of [Zn(ENTPP)($H_2O$)] · $C_6H_5CH_3$ has been solved in the $P\bar{1}$ space group, and one asymmetric unit consists of two independent zinc porphyrinate molecules and two

Table 1. Crystallographic data for [Zn(ENTPP)($CH_3OH$)] and [Zn(ENTPP)($H_2O$)] · $C_6H_5CH_3$.

| Crystal | [Zn(ENTPP)($CH_3OH$)] | [Zn(ENTPP)($H_2O$)] · $C_6H_5CH_3$ |
|---|---|---|
| Empirical formula | $C_{52}H_{38}N_4O_3Zn$ | $C_{116}H_{88}N_8O_6Zn_2$ |
| Formula weight | 832.23 | 1820.68 |
| Crystal system | Monoclinic | Triclinic |
| Space group | $P2(1)/c$ | $P\bar{1}$ |
| Temperature (K) | 223(2) | 293(2) |
| Unit cell dimensions (Å, °) | | |
| $a$ | 14.525(3) | 13.078(3) |
| $b$ | 11.125(2) | 17.370(4) |
| $c$ | 25.615(5) | 22.840(5) |
| $\alpha$ | 90 | 77.39(3) |
| $\beta$ | 100.82(3) | 73.74(3) |
| $\gamma$ | 90 | 76.12(3) |
| Volume (Å$^3$), $Z$ | 4065.2(14), 4 | 4771.6(17), 2 |
| Calculated density (g cm$^{-3}$) | 1.360 | 1.267 |
| Absorption coefficient (mm$^{-1}$) | 0.655 | 0.564 |
| $F$(000) | 1728 | 1896 |
| Reflections collected | 21,995 | 44,281 |
| Independent reflections | 7078 [$R$(int) = 0.0521] | 16,711 [$R$(int) = 0.0304] |
| Parameters | 543 | 1317 |
| Goodness-of-fit | 1.079 | 1.072 |
| $R_1$ [$I > 2\sigma(I)$] | 0.0774 | 0.0594 |
| $wR_2$ (all data) | 0.1982 | 0.1518 |

$R_1 = \Sigma(||F_o| - |F_c||)/\{\Sigma|F_o\}$, $wR_2 = \Sigma w(|F_o|^2 - |F_c|^2)^2/[\Sigma w(|F_o|^2)^2]^{1/2}$.

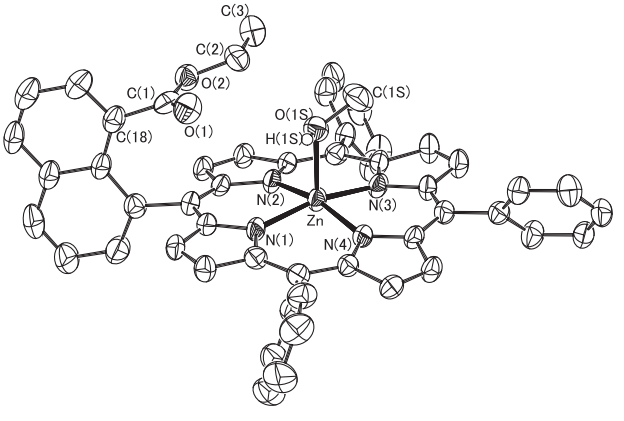


Figure 1. ORTEP view for [Zn(ENTPP)($CH_3OH$)] at 50% probability thermal ellipsoids. The hydrogen atoms except H(1S) have been omitted for clarity.

toluene solvates. Their ORTEP diagrams are presented in figures 1 and 2. In the porphyrin, there are three phenyl groups and one naphthyl group at mesopositions. Zinc is five-coordinate in both cases, the axial ligands are methanol and water, respectively. The corresponding distance Zn–O is 2.155(4) Å for [Zn(ENTPP)($CH_3OH$)], 2.145(2) Å and 2.233(2) Å for [Zn(ENTPP)($H_2O$)] · $C_6H_5CH_3$; other related distances are listed in table 2. These distances are similar to the corresponding distances in [Zn(SATPP)($CH_3OH$)] [4], [Zn(TPP)($CH_3OH$)] [8], [Zn(TPP)($H_2O$)] [9], [Zn($C_{45}H_{28}N_4O_2$)($H_2O$)] · $2C_6H_5NO_2$ [10], ($C_{45}H_{28}N_4O_2$, dianion of 20-(4-carboxyphenyl)-5,10,15-triphenylporphyrin)), [Zn($C_{48}H_{48}N_4O_3$)($H_2O$)] [11], ($C_{48}H_{48}N_4O_3$, dianion

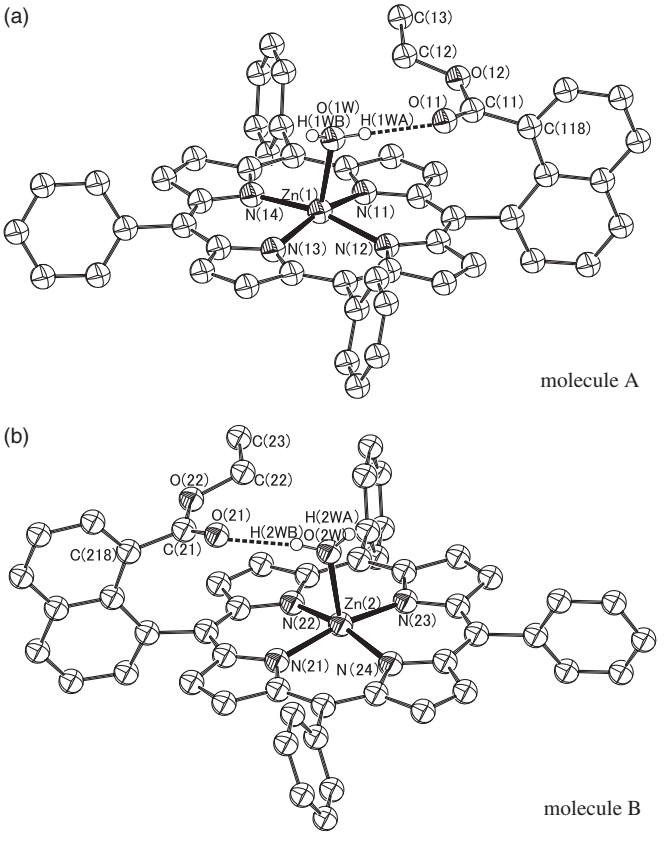


Figure 2. ORTEP view for $[Zn(ENTPP)(H_2O)] \cdot C_6H_5CH_3$ at 50% probability thermal ellipsoids: (a) molecule A consisting of Zn(1); (b) molecule B consisting of Zn(2). The hydrogen atoms except H(1S), H(1WA), H(1WB), H(2WA), and H(2WB) have been omitted for clarity.

Table 2. Selected bond lengths (Å) for $[Zn(ENTPP)(CH_3OH)]$ and $[Zn(ENTPP)(H_2O)] \cdot C_6H_5CH_3$.

| $[Zn(ENTPP)(CH_3OH)]$ | | $[Zn(ENTPP)(H_2O)] \cdot C_6H_5CH_3$ | | | |
|---|---|---|---|---|---|
| Zn–N(1) | 2.049(4) | Zn(1)–N(11) | 2.064(3) | Zn(2)–N(21) | 2.051(3) |
| Zn–N(2) | 2.066(4) | Zn(1)–N(12) | 2.061(3) | Zn(2)–N(22) | 2.063(3) |
| Zn–N(3) | 2.054(4) | Zn(1)–N(13) | 2.066(3) | Zn(2)–N(23) | 2.054(3) |
| Zn–N(4) | 2.063(4) | Zn(1)–N(14) | 2.059(3) | Zn(2)–N(24) | 2.053(3) |
| Zn–O(1) | 2.155(4) | Zn(1)–O(1W) | 2.145(2) | Zn(2)–O(2W) | 2.233(2) |
| C(1)–C(18) | 1.511(8) | C(11)–C(118) | 1.502(5) | C(21)–C(218) | 1.499(4) |
| C(2)–C(3) | 1.483(8) | C(12)–C(13) | 1.487(6) | C(22)–C(23) | 1.503(6) |
| C(1)–O(1) | 1.207(6) | C(11)–O(11) | 1.198(4) | C(21)–O(21) | 1.212(4) |
| C(1)–O(2) | 1.334(7) | C(11)–O(12) | 1.326(4) | C(21)–O(22) | 1.330(4) |
| C(2)–O(2) | 1.461(6) | C(12)–O(12) | 1.446(5) | C(22)–O(22) | 1.466(6) |
| C(1S)–O(1S) | 1.415(7) | | | | |

of 5-(5-carboxy-9,9-dimethyl-(9H)-xanthen-4-yl)-2,8,13,17-tetraethyl3,7,12,18-tetramethylporphyrin). As five-coordinate species, zinc is not within the porphyrin plane, but out of four pyrrole nitrogen plane with displacements 0.26 Å for $[Zn(ENTPP)(CH_3OH)]$, 0.27 Å for molecule A, and 0.24 Å for molecule B in

Table 3. Hydrogen-bonds lengths (Å) and angles (°) for [Zn(ENTPP)($CH_3OH$)] and [Zn(ENTPP)($H_2O$)]·$C_6H_5CH_3$.

| D–H···A | *d*(D–H) | *d*(H···A) | *d*(D···A) | ∠(DHA) |
|---|---|---|---|---|
| [Zn(ENTPP)($CH_3OH$)] | | | | |
| O(1 S)–H(1 S)···O(1 S#1) | 0.820(4) | 2.019(6) | 2.788(6) | 155(8) |
| [Zn(ENTPP)($H_2O$)]·$C_6H_5CH_3$ | | | | |
| O(2W)–H(2WB)···O(21) | 0.850(10) | 2.023(12) | 2.861(4) | 168(4) |
| O(1W)–H(1WA)···O(11) | 0.848(10) | 2.045(16) | 2.835(3) | 155(3) |
| O(1W)–H(1WB)···O(21#2) | 0.849(10) | 1.981(12) | 2.818(3) | 169(3) |

Symmetry operator #1: $x$, $1.5-y$, $0.5+z$; #2: $-x$, $-y$, $1-z$.



[Zn(ENTPP)($H_2O$)]·$C_6H_5CH_3$, respectively. Diagrams showing atomic displacements from the mean plane of the four nitrogen core are given in the "Supplementary material."

Our focus is the role of axial ligand in their structures. The methanol (or water) molecule is not only coordinated to zinc, but also involved in hydrogen-bonding interactions. In [Zn(ENTPP)($CH_3OH$)], the methanol forms an intermolecular hydrogen bond with the carboxylate oxygen in a symmetry related molecule (symmetry operator #1: $x$, $1.5-y$, $0.5+z$). The corresponding O(3)···O(1#1) distance is 2.788(6) Å. Related distances and angles are listed in table 3. Because of this hydrogen bond, one porphyrin packs with its symmetry related neighboring molecule to build a dimer as shown in figure 3(a).

For [Zn(ENTPP)($H_2O$)]·$C_6H_5CH_3$, the hydrogen-bonding pattern is more complicated. Water in the two independent molecules is involved in different hydrogen-bonding interactions. For molecule B, there is an intramolecular hydrogen bond between water oxygen and carboxylate oxygen in the naphthyl group with O(2W)···O(21) distance 2.835(3) Å, while in molecule A, instead of one hydrogen bond, the coordinated water is involved in two hydrogen bonds, one an intramolecular hydrogen bond between water oxygen and carboxylate oxygen in the naphthyl group and the other is an intermolecular hydrogen bond between water oxygen and carboxylate oxygen of an adjacent molecule (symmetry operator #2: $-x$, $-y$,$1-z$). The corresponding distance of O(1W)···O(11) is 2.861(4) Å and O(1W)···O(21#2) is 2.818(3) Å. These two molecules form a dimer through such hydrogen bonds as shown in figure 3(b). The above structural results suggest that ENTPP is capable of forming hydrogen bonds with a coordinated ligand.

In these [Zn(ENTPP)] complexes, the hydrogen-bonding patterns are much different from that in [Zn(SATPP)($CH_3OH$)]. Considering the structural features of ENTPP, steric effect causes the O(1)–C(1)–O(2) plane to be nearly parallel to the porphyrin plane. This geometry makes the carbonyl oxygen tilt away from porphyrin center, close to the porphyrin edge. Such arrangement could weaken the intramolecular hydrogen bond between the carboxylate oxygen and the coordinated ligand. On the other hand, such arrangement allows the carboxylate oxygen to have more space to form intermolecular hydrogen bonds with neighboring molecule. That is also a possible reason to form dimers through hydrogen-bonding in these [Zn(ENTPP)] species.

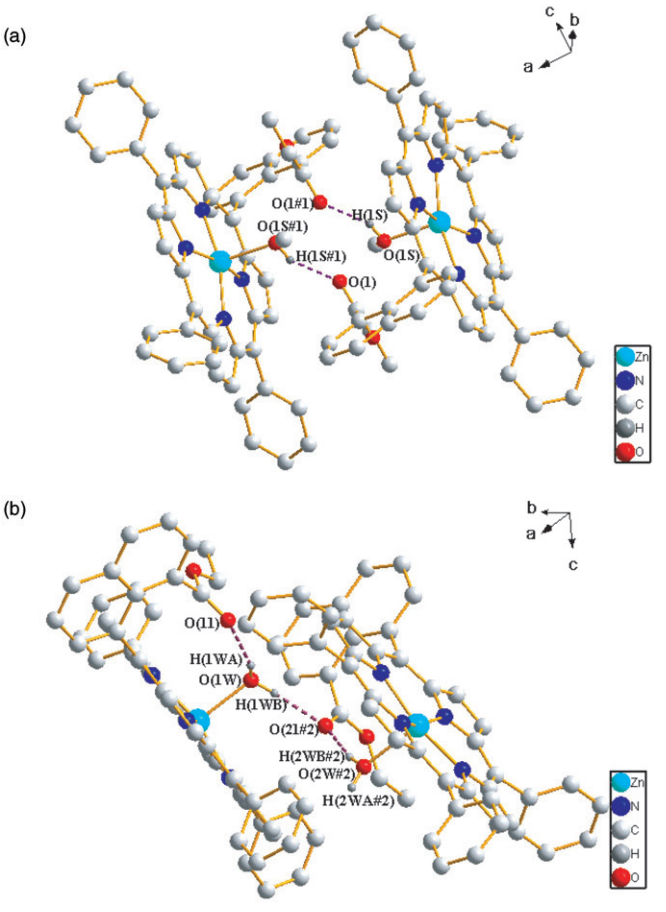


Figure 3. (a) Diagram of dimer in [Zn(ENTPP)($CH_3OH$)] formed by intermolecular hydrogen-bonding interactions and (b) diagram of dimer in [Zn(ENTPP)($H_2O$)] · $C_6H_5CH_3$ formed by both intermolecular and intramolecular hydrogen-bonding interactions.

### 3.2. *$^1$H NMR spectra*

For porphyrins, NMR provides a very useful probe of intramolecular interactions due to the ring current effect [12]. The $^1$H NMR spectra of [Zn(ENTPP)($CH_3OH$)] in the selected region in $CDCl_3$ are shown in figure 4(a). Binding of methanol and water to zinc are verified by $^1$H NMR studies in solution. When methanol is coordinated to zinc, methanol protons are in the shielding region and the ring current effect will cause a remarkable upfield shift. Such shift is evidenced by the resonances of methanol proton at 2.44 and 0.24 ppm as shown in figure 4(b). Compared with free methanol, these resonances shift upfield by 1.05 and 0.85 ppm, respectively. Notably, there is another signal at 1.06 ppm, which is assigned to the water protons. In $CDCl_3$, $H_2O$ is a common impurity which usually has a resonance at 1.56 ppm. But in our case, when it is coordinated to zinc in solution, its resonance shifts upfield by 0.50 ppm. So there are two equilibria involved in the solution as shown in scheme 2. The resonances observed

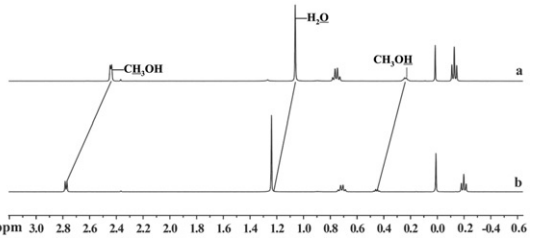


Figure 4. $^1$H NMR spectra of $[Zn(ENTPP)(CH_3OH)]\cdot C_6H_5CH_3$ in the selected region in $CDCl_3$: (a) the concentrated solution and (b) the diluted solution.

$$[Zn\ (ENTPP)] + CH_3OH \underset{}{\overset{K_1}{\rightleftharpoons}} [Zn\ (ENTPP)(CH_3OH)] \quad (1)$$

$$[Zn\ (ENTPP)] + H_2O \underset{}{\overset{K_2}{\rightleftharpoons}} [Zn\ (ENTPP)(H_2O)] \quad (2)$$

Scheme 2. The equilibria between four-coordinate and five-coordinate porphyrin complexes in solution.

are actually the average contribution from both coordinated and uncoordinated $CH_3OH$ (or $H_2O$). These equilibria are further confirmed by concentration-dependent $^1$H NMR spectra. The spectrum of the diluted solution is shown in figure 4(b). The resonances of methanol shift downfield by 0.34 and 0.22 ppm and that of water shifts downfield by 0.18 ppm. It can be explained as the following reason: the equilibrium (1) will be driven to the reverse reaction when the concentrations of both reactants decrease; it will eventually increase the ratio of uncoordinated to coordinated methanol, which causes the corresponding proton resonances to shift downfield. In the case of water, because the ratio of uncoordinated to coordinated water increases as the amount of uncoordinated $H_2O$ increases, the average $H_2O$ resonance shifts downfield.

### 3.3. *UV-Vis spectra*

The binding constant $K_1$ for equilibrium (1) can be measured by UV-Vis spectroscopy according to a method in the literature [13]. Titration of [Zn(ENTPP)] with methanol has been performed and is shown in figure 5. The following double reciprocal relationship can be defined [14]:

$$\frac{1}{\Delta A} = \frac{1}{K\Delta A_\infty} \times \frac{1}{[CH_3OH]} + \frac{1}{\Delta A_\infty}, \quad (3)$$

where $1/\Delta A$ is the reciprocal of the change in absorbance observed after the addition of methanol to a [Zn(ENTPP)] solution and $\Delta A_\infty$ is the reciprocal of the *y*-intercept obtained in equation (1) yielding the absorbance change observed at infinite ligand concentrations. $1/\Delta A$ is plotted *versus* the reciprocal of the added ligand concentration, $1/[L]$. The linear least-squares analysis [15] is used to evaluate the slope and *y*-intercept of the plotted data, given in figure S3. The obtained slope is 0.0788 which gives the $K_1$ for the equilibrium as 40.6 L mol$^{-1}$. Such binding constant is over four times larger than the corresponding value for [Zn(TPP)] [13]. Considering the hydrogen-bonding

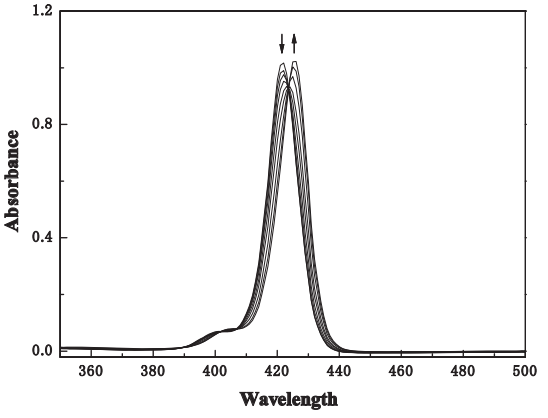


Figure 5. Spectral changes occurring upon titration of a [Zn(ENTPP)] solution with methanol. Porphyrin concentration: $1.78 \times 10^{-5}$ mol $L^{-1}$. Spectrum recorded at 25°C with dichloromethane as the solvent. In the titration, each step represents the following ligand concentrations (mol $L^{-1}$) increasing in the direction of the arrow: 0, $1.85 \times 10^{-3}$, $3.70 \times 10^{-3}$, $6.16 \times 10^{-3}$, $1.23 \times 10^{-2}$, $1.85 \times 10^{-2}$, $0.41 \times 10^{-2}$, $1.37 \times 10^{-1}$, and $1.23 \times 10^{-1}$. The absorbance intensities at 422 nm were used for the linear least-squares analysis.

interactions, it is possible that the hydrogen bond moderately increases the binding ability of methanol to zinc in [Zn(ENTPP)($CH_3OH$)].

The attempt to measure binding constant $K_2$ for the equilibrium (2) has also been performed in toluene. But there was no observable shift. The possible reason could be the limited solubility of water and small binding constant.

## 4. Conclusion

We have synthesized two mononaphthyl porphyrin complexes, [Zn(ENTPP)($CH_3OH$)] and [Zn(ENTPP)($H_2O$)] · $C_6H_5CH_3$. X-ray crystallography shows that in the structure of [Zn(ENTPP)($CH_3OH$)], the methanol oxygen and the carboxylate oxygen in the naphthyl group form an intermolecular hydrogen bond. In molecule B of [Zn(ENTPP)($H_2O$)] · $C_6H_5CH_3$, there is an intramolecular hydrogen bond between the water oxygen and the carboxylate oxygen; while in molecule A, besides the intramolecular hydrogen bond, there is an intermolecular hydrogen bond between the water oxygen and the carboxylate oxygen. The structural result proves that such naphthyl substituted porphyrin is capable of forming a hydrogen bond with a coordinated molecule. For [Zn(SATPP)] species, the phenol oxygen is located along the center position, which could make it much closer to the ligand, leading to strong intramolecular hydrogen bonds. While in both [Zn(ENTPP)] structures, the carbonyl oxygen is tilted away from the porphyrin center, weakening the intramolecular hydrogen bonds with the ligand and making carbonyl oxygen much easier to form intermolecular hydrogen bonds with neighboring molecules. This is consistent with a smaller binding constant for [Zn(ENTPP)] than for [Zn(SATPP)].

## Supplementary material

Figures S1 and S2 display the displacements from four pyrrole nitrogen plane. Figures S3 and S4 display the full $^1$H NMR spectra at different concentrations. Figure S5 gives the linear fit for equation (1). Tables S1 and S2 give complete crystallographic details, atomic coordinates, bond distances and angles, anisotropic temperature factors, and fixed hydrogen atom positions. CCDC 860474 and 860475 contain the supplementary crystallographic data. These data can be obtained free of charge *via* www.ccdc.cam.ac.uk/conts/retrieving.html or by application to The Director, CCDC, 12 Union Road, Cambridge CB2 1EZ, UK; Fax: (+44) 1223 336 033; E-mail: deposit@ccdc.cam.ac.uk.



## Acknowledgments

This work was supported by the Natural Science Foundation of China (No. 20971093) and the Priority Academic Program Development of Jiangsu Higher Education Institutions.

## References

[1] T. Hayashi, T. Miyahara, N. Hashizume, H. Ogoshi. *J. Am. Chem. Soc.*, **115**, 2049 (1993); (b) T. Mizutani, T. Ema, T. Yoshida, Y. Kuroda, H. Ogoshi. *Inorg Chem.*, **32**, 2072 (1993); (c) H. Ogoshi, T. Mizutani. *Acc. Chem. Res.*, **31**, 81 (1998); (d) G.A. Hembury, V.V. Borovkov, Y. Inoue. *Chem. Rev.*, **108**, 1 (2008).
[2] Y. Aoyama, M. Asakawa, Y. Matsui, H. Ogoshi. *J. Am. Chem. Soc.*, **113**, 6233 (1991).
[3] (a) C. Hu, B.C. Noll, P.M.B. Piccoli, A.J. Schultz, C.E. Schulz, W.R. Scheidt. *J. Am. Chem. Soc.*, **130**, 3127 (2008); (b) C. Hu, B.C. Noll, C.E. Schulz, W.R. Scheidt. *Inorg. Chem.*, **47**, 8884 (2008).
[4] W. Huang, J.X. Jiang, Z.Q. Feng, X.X. Kai, C.J. Hu, H. Yu, W. Yang. *J. Coord. Chem.*, **64**, 2101 (2011).
[5] J.X. Yang, J.X. Jiang, W.G. Fang, X.X. Kai, C.J. Hu, Y.G. Yang. *J. Porphyrins Phthalocyanines*, **15**, 197 (2011).
[6] T. Chandra, B.J. Kraft, J.C. Huffman, J.M. Zaleski. *Inorg. Chem.*, **42**, 5158 (2003).
[7] G.M. Sheldrick. *SHELXL-97, Program for the Refinement of Crystal Structure*, University of Göttingen, Germany (1997).
[8] J. Nakazawa, M. Mizuki, J. Hagiwara, Y. Shimazaki, F. Tani, Y. Naruta. *Bull. Chem. Soc. Japan*, **79**, 1431 (2006).
[9] A.J. Golder, D.C. Porey, J. Silver, Q.A.A. Jassim. *Acta Cryst.*, **C46**, 1210 (1990).
[10] S. Lipstman, S. Muniappan, I. Goldberg. *Acta Cryst.*, **C62**, m538 (2006).
[11] C.K. Chang, N. Bag, B.M. Guo, S.M. Peng. *Inorg. Chim. Acta*, **351**, 261 (2003).
[12] C.J. Medforth. In *The Porphyrin Handbook*, K. Kadish, K. Smith, R. Guilard (Eds), Vol. 5, pp. 1–80, Academic Press, New York (2000).
[13] J.V. Nardo, J.H. Dawson. *Inorg. Chim. Acta*, **123**, 9 (1986).
[14] J.V. Nardo, J.H. Dawson. *Spectrosc. Int. J.*, **2**, 326 (1983).
[15] N.R. Draper, H. Smith. *Applied Regression Analysis*, 2nd Edn, Wiley, New York (1981).